We are IntechOpen,
the world's leading publisher of
Open Access books
Built by scientists, for scientists

5,300
Open access books available

131,000
International authors and editors

160M
Downloads

154
Countries delivered to

Our authors are among the

TOP 1%
most cited scientists

12.2%
Contributors from top 500 universities

BOOK CITATION INDEX
CLARIVATE ANALYTICS
INDEXED

WEB OF SCIENCE™

Selection of our books indexed in the Book Citation Index
in Web of Science™ Core Collection (BKCI)

Interested in publishing with us?
Contact book.department@intechopen.com

Numbers displayed above are based on latest data collected.
For more information visit www.intechopen.com

Modeling of Photovoltaic Grid Connected Inverters Based on Nonlinear System Identification for Power Quality Analysis

Nopporn Patcharaprakiti[1,2], Krissanapong Kirtikara[1,2],
Khanchai Tunlasakun[1], Juttrit Thongpron[1,2], Dheerayut Chenvidhya[1],
Anawach Sangswang[1], Veerapol Monyakul[1] and Ballang Muenpinij[1]
[1]King Mongkut's University of Technology Thonburi, Bangkok,
[2]Rajamangala University of Technology Lanna, Chiang Mai
Thailand

1. Introduction

Photovoltaic systems are attractive renewable energy sources for Thailand because of high daily solar irradiation, about 18 MJ/m²/day. Furthermore, renewable energy is boosted by the government incentive on adders on electricity from renewable energy like solar PV, wind and biomass, introduced in the second half of 2000s. For PV systems, domestic rooftop PV units, commercial rooftop PV units and ground-based PV plants are appealing. Applications of electricity supply from PV plants that have been filed total more than 1000 MW. With the adder incentive, more households will be attracted to produce electricity with a small generating capacity of less than 10 kW, termed a very small power producer (VSPP). A possibility of expanding domestic roof-top grid-connected units draw our attention to study single phase PV-grid connected systems. Increased PV penetration can have significant [1-2] and detrimental impacts on the power quality (PQ) of the distribution networks [3-5]. Fluctuation of weather condition, variations of loads and grids, connecting PV-based inverters to the power system, requires power quality control to meet standards of electrical utilities. PV can reduce or improve power quality levels [6-9]. Different aspects should be taken into account. In particular, large current variations during PV connection or disconnection can lead to significant voltage transients [10]. Cyclic variations of PV power output can cause voltage fluctuations [11]. Changes of PV active and reactive power and the presence of large numbers of single phase domestic generators can lead to long-duration voltage variations and unbalances [12]. The increasing values of fault currents modify the voltage sag characteristics. Finally, the waveform distortion levels are influenced in different ways according to types of PV connections to the grid, i.e. direct connection or by power electronic interfaces. PV can improve power quality levels, mainly as a consequence of increase of short circuit power and of advanced controls of PWM converters and custom devices. [13]

Grid-connected inverter technology is one of the key technologies for reliable and safety grid interconnection operation of PV systems [14-15]. An inverter being a power

conditioner of a PV system consists of power electronic switching components, complex control systems [16]. In addition, their operations depends on several factors such as input weather condition, switching algorithm and maximum power point tracking (MPPT) algorithm implemented in grid-connected inverters, giving rise to a variety of nonlinear behaviors and uncertainties [17]. Operating conditions of PV based inverters can be considered as steady state condition [18], transient condition [19-20], and fault condition such islanding [21-22]. In practical operations, inverters constantly change their operating conditions due to variation of irradiances, temperatures, load or grid impedance variations. In most cases, behavior of inverters is mainly considered in a steady state condition with slowly changing grid, load and weather conditions. However, in many instances conditions suddenly change, e.g. sudden changes of input weather, cloud or shading effects, loads and grid changes from faults occurring in near PV sites [23]. In these conditions, PV based inverters operate in transient conditions. Their average power increases or decreases upon the disturbances to PV systems [24]. In order to understand the behavior of PV based inverters, modeling and simulation of PV based inverter systems is the one of essential tools for analysis, operation and impacts of inverters on the power systems [25].

There are two major approaches for modeling power electronics based systems, i.e. analytical and experimental approaches. The analytical methods to study steady state, transient models and islanding conditions of PV based inverter systems, such as state space averaging method [26], graphical techniques [27-28] and computation programming [29]. In using these analytic methods, one needs to know information of system. However, PV based inverters are usually commercial products having proprietary information; system operators do not know the necessary information of products to parameterize the models. In order to build models for nonlinear devices without prior information, system identification methods are exposed [33-34]. In the method reported in this paper, specific information of inverter is not required in modeling. Instead, it uses only measured input and output waveforms.

Many recent research focuses on identification modeling and control for nonlinear systems [35-37]. One of the effective identification methods is block oriented nonlinear system identification. In the block oriented models, a system consists of numbers of linear and nonlinear blocks. The blocks are connected in various cascading and parallel combinations representing the systems. Many identification methods of well known nonlinear block oriented models have been reported in the literature [38-39]. They are, for example, a NARX model [40], a Hammerstein model [41], a Wiener model [42], a Wiener-Hammerstein model and a Hammerstein-Wiener model [43]. Advantages of a Hammerstein model and a Wiener model enables combination of both models to represent a system, sensors and actuators in to one model. The Hammerstein-Wiener model is recognized as being the most effective for modeling complex nonlinear systems such PV based inverters [44].

In this paper, real operating conditions weather input variation, i.e. load variations and grid variations, of PV- based inverters are considered. Then two different experiments, steady state and transient condition, are designed and carried out. Input-output data such as currents and voltages on both dc and ac sides of a PV grid-connected systems are recorded. The measured data are used to determine the model parameters by a Hammerstein-Wiener nonlinear model system identification process. In the Section II, PV system characteristics are introduced. The I-V characteristic, an equivalent model, effects of radiation and temperature on voltage and current of PV are described. In the Section III, system identification methods, particularly a Hammerstein-Wiener Model is explained. In the

following section, the experimental design and implementation to model the system is illustrated. After that, the obtained model from prior sections is analyzed in terms of control theories. In the last section, the power quality analysis is discussed. The output prediction is performed to obtain electrical outputs of the model and its electrical power. The power quality nature is analyzed for comparison with outputs of model. Subsequently, voltage and current outputs from model are analyzed by mathematical tools such the Fast Fourier Transform-FFT, the Wavelet method in order to investigate the power quality in any operating situations.

2. PV grid connected system (PVGCS) operation

In this section, PV grid connected structures and components are introduced. Structures of PBGCS consist of solar array, power conditioners, control systems, filtering, synchronization, protection units, and loads, shown in Fig. 1.
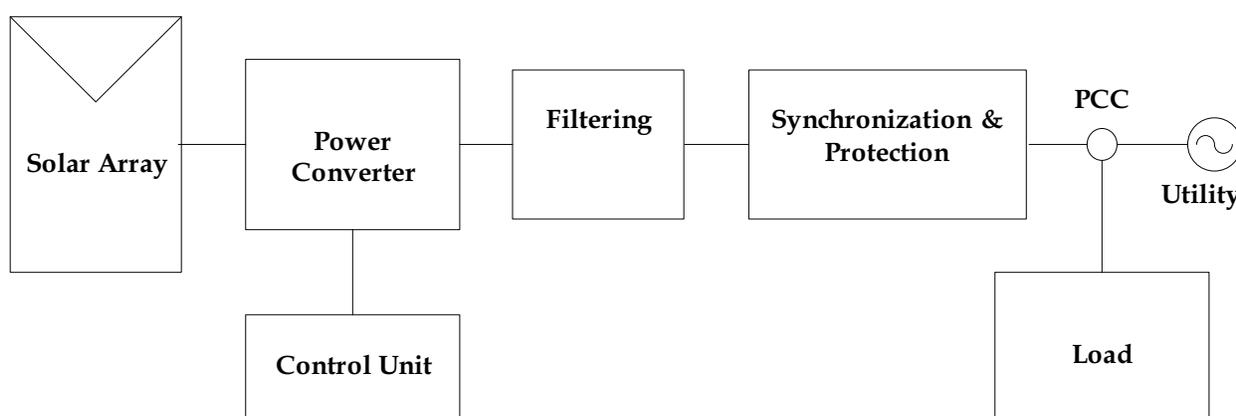

Fig. 1. Block diagram of a PV grid connected system

2.1 Solar array
Environmental inputs affecting solar array/cell outputs are temperature (T) and irradiance (G), fluctuating with weather conditions. When the ambient temperature increases, the array short circuit current slight increases with a significant voltage decrease. Temperature and I-V characteristics are related, characterized by array/cell temperature coefficients. Effects of irradiance, radiant solar energy flux density in W/m^2, apart from solar radiation at sea level, are determined by incident angles and array/cell envelops. Typical characteristics of relationship between environmental inputs (irradiance and temperature) and electrical parameters (current and voltage of array/cells) are shown in Fig. 2 [45]. In our experimental designs, operating conditions of PV systems under test is designed and based on typical operating conditions.

2.2 Operating conditions of a PV grid connected system
A PV system, generating power and transmitting it into the utility, can be categorized in three cases, i.e. a steady state condition, a transient condition and a fault condition like islanding. Three factors affecting the operation of inverters are input weather conditions, local loads and utility grid variations.
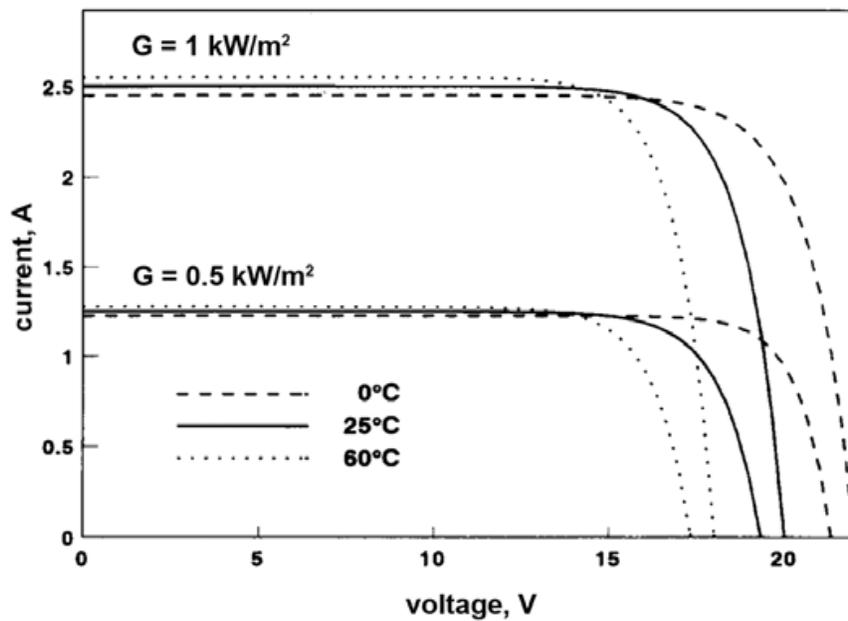
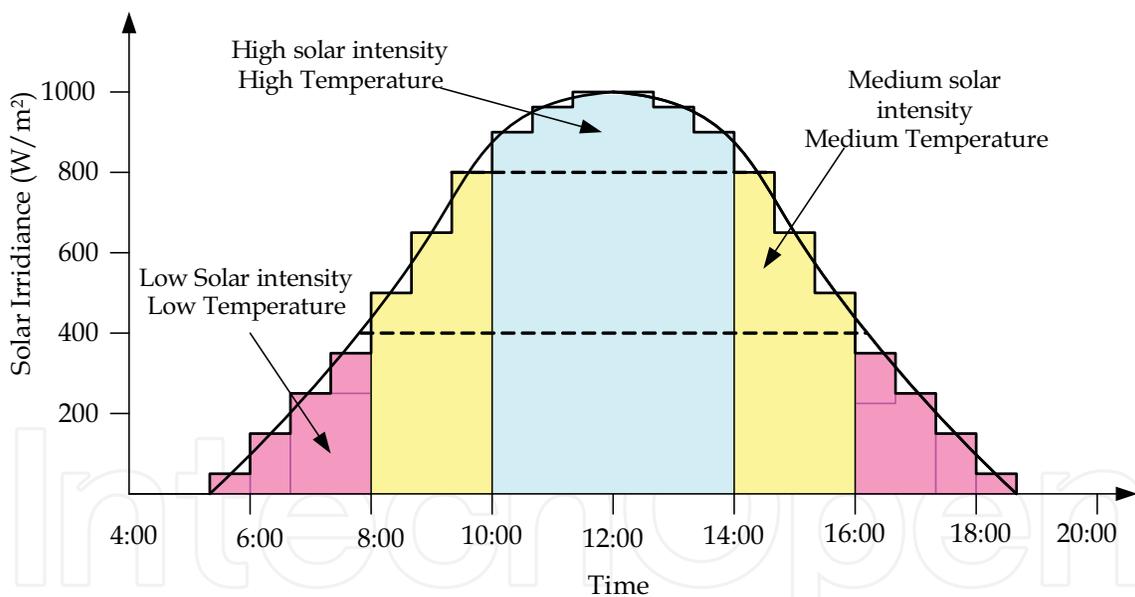Fig. 2. Temperature and irradiance effects on I-V characteristics of PV arrays/cells [46]

Fig. 3. Variations of solar irradiance and temperature throughout a day conditioning PVGCS operation

Firstly, under a steady state condition, input, load and utility under consideration are treated as being constant with slightly change weather condition. Installed capacities of PV systems in a steady state are low, medium and high capacity. According to the weather conditions throughout a day as shown in Fig. 3 [47-48], a low radiation about 0-400 W/m² is common in an early morning (6:00 AM-9:00 AM) and early evening (16:00 PM-19:00 PM), medium radiation of 400-800 W/m² in late morning (9:00 AM-11:00 PM) and early afternoon (14:00 PM-16:00 PM) and high radiation of 800-1000 W/m² around noon (11.00

AM - 14:OO PM). Loads fluctuate upon activities of customer groups, for example, a peak load for industrial zones occurs in afternoon (13:00 - 17:00 PM) and a peak load for residential zones occurs in evening(18:00 - 21:00 PM). Variations from steady state conditions impact power quality such as overvoltage, over-current, harmonics, and so on. In case of transients, there are variations in inputs, loads and utility. Weather variations such solar irradiance and temperature exhibit significant changes. Unexpected accidents happen. Local loads may sudden change due to activities of customers in each time. A utility has some faults in nearby locations which impact utility parameters such grid impedance. These conditions lead to short duration power quality problems with such spikes, voltage sag, voltage swell. In some extreme cases, abnormal conditions, such as very low solar irradiance or abnormal conditions such islanding, the gird-connected PV systems may collapse. The PV systems are black out and cut out of the utility grid. Such can affect power quality, stability and reliability of power systems.

2.3 Power converter

There are several topologies for converting a DC to DC voltage with desired values, for example, Push-Pull, Flyback, Forward, Half Bridge and Full Bridge [49]. The choice for a specific application is often based on many considerations such as size, weight of switching converter, generation interference and economic evaluation [50-51]. Inverters can be classified into two types, i.e. voltage source inverter (VSI) if an input voltage remains constant and a current source inverter (CSI) if input current remains constant [52-53]. The CSI is mostly used in large motor applications, whereas the VSI is adopted for and alone systems. The CSI is a dual of a VSI. A control technique for voltage source inverters consists of two types, a voltage control inverter, shown in Fig. 4(a) and a current control inverter, Fig. 4(b) [54].
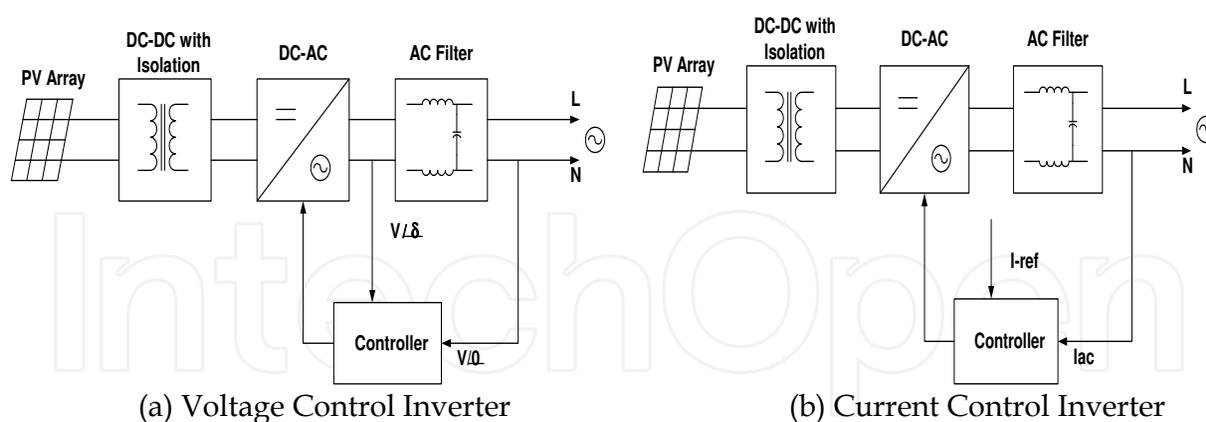

(a) Voltage Control Inverter   (b) Current Control Inverter

Fig. 4. Control techniques for an inverter

3. System Identification

System identification is the process for modeling dynamical systems by measuring the input/output from system. In this section, the principle of system identification is described. The classification is introduced and particularly a Hammerstein-Wiener model is explained. Finally, a MIMO (multi input multi output model with equation and characteristic is illustrated.

3.1 Principle of system identification

A dynamical system can be classified in terms of known structures and parameters of the system, shown in Fig.5, and classified as a "White Box" if all structures and parameters are known, a "Grey Box" , if some structures and parameters known and a "Black Box" if none are known [55].
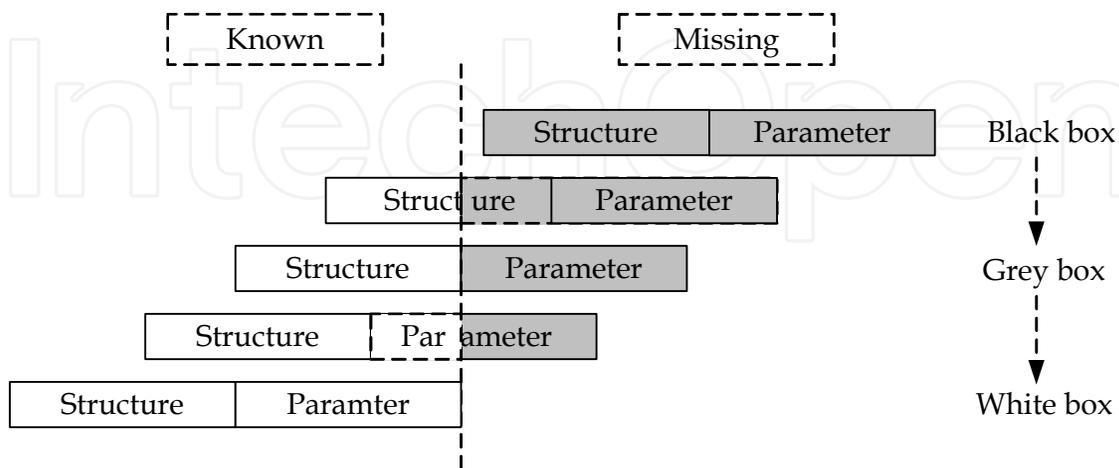

Fig. 5. Dynamical system classifications by structures and parameters

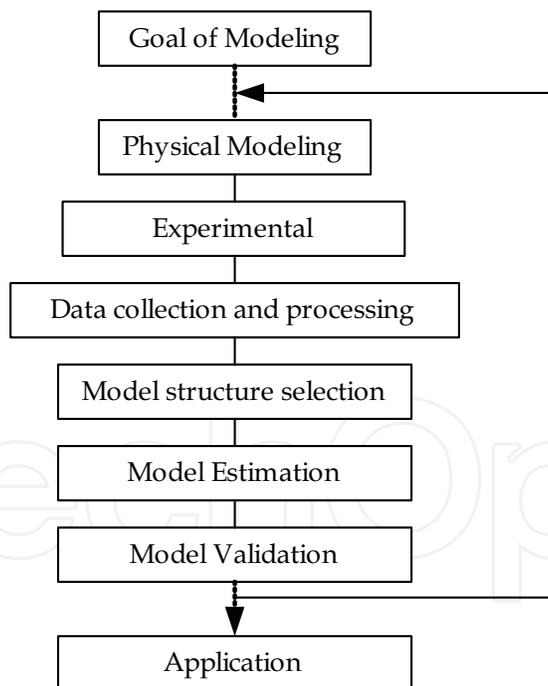Steps in system identification can be described as the following process, shown in Fig. 6.

Fig. 6. System identification processes

Each step can be described as follows

3.1.1 Goal of modeling

The primary goal of modeling is to predict behaviors of inverters for PV systems or to simulate their outputs and related values. The other important goal is to acquire

mathematical and physical characteristics and details of systems for the purposes of controlling, maintenance and trouble shooting of systems, and planning of managing the power system.

3.1.2 Physical modeling

Photovoltaic inverters, particularly commercial products, compose of two parts, i.e. a power circuit and a control circuit. Power electronic components convert, transfer and control power from input to output. The control system, switching topologies of power electronics are done by complex digital controls.

3.1.3 Model structure selection

Model structure selection is the stage to classify the system and choose the method of system identification. The system identification can be classified to yield a nonparametric model and a parametric model, shown in Fig 7. A nonparametric model can be obtained from various methods, e.g. Covariance function, Correlation analysis. Empirical Transfer Function Estimate and Periodogram, Impulse response, Spectral analysis, and Step response.
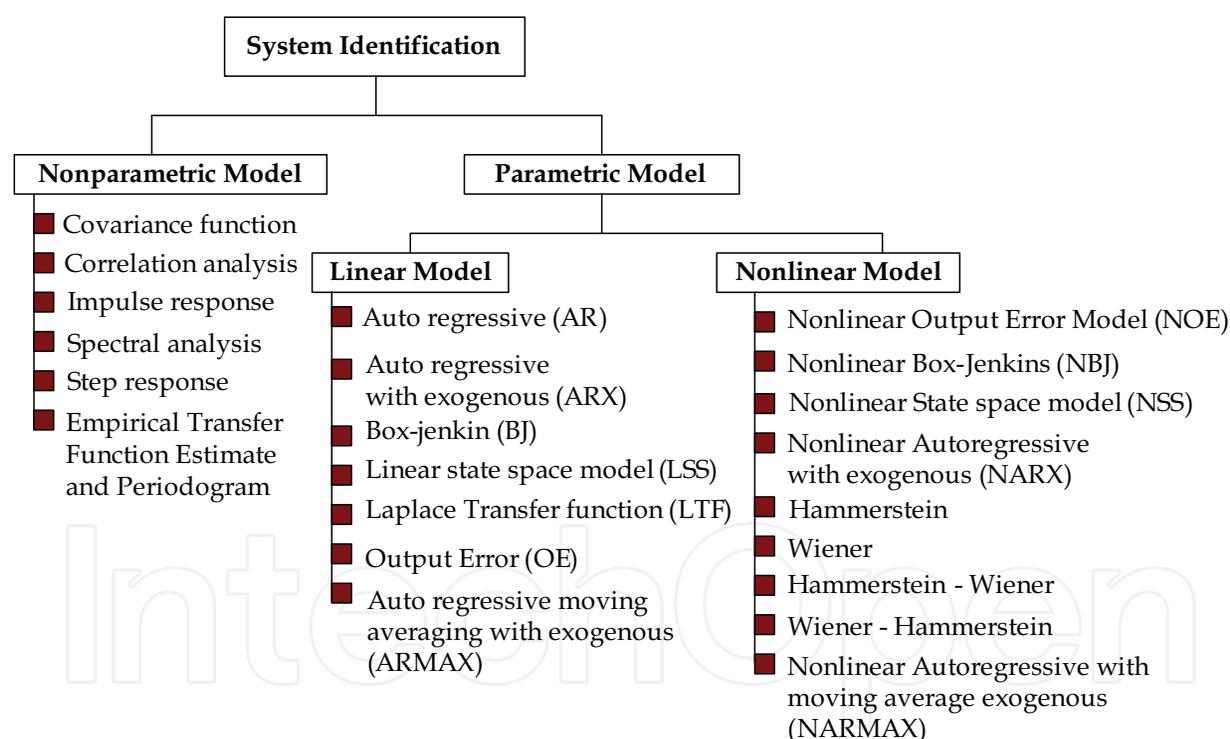

Fig. 7. Classification of system identification

Parametric models can be divided to two groups: linear parametric models and nonlinear parametric models. Examples of linear parametric models are Auto Regressive (AR), Auto Regressive Moving Average (ARMA), and Auto Regressive with Exogenous (ARX), Box-Jenkins, Output Error, Finite Impulse Response (FIR), Finite Step Response (FSR), Laplace Transfer Function (LTF) and Linear State Space (LSS). Examples of nonlinear parametric models are Nonlinear Finite Impulse Response (NFIR), Nonlinear Auto-Regressive with Exogenous (NARX), Nonlinear Output Error (NOE), and Nonlinear Auto-Regressive with

Moving Average Exogenous (NARMAX), Nonlinear Box-Jenkins (NBJ), Nonlinear State Space, Hammerstein model, Wiener Model, Hammerstein-Wiener model and Wiener-Hammerstein model [56]. In practice, all systems are nonlinear; their outputs are a nonlinear function of the input variables. A linear model is often sufficient to accurately describe the system dynamics as long as it operates in linear range Otherwise a nonlinear is more appropriate. A nonlinear model is often associated with phenomena such as chaos, bifurcation and irreversibility. A common approach to nonlinear problems solution is linearization, but this can be problematic if one is trying to study aspects such as irreversibility, which are strongly tied to nonlinearity. Inverters of PV systems can be identified based on nonlinear parametric models using various system identification methods.

3.1.4 Experimental design

The experimental design is an important stage in achieving goals of modeling. Number parameters such as sampling rates, types and amount of data should be concerned. Grid connected inverters have four important input/output parameters, i.e. DC voltage (Vdc), DC current voltage (Idc), AC voltage (Vac) and AC current (Iac). In experiments, these data are measured, collected and send to a system identification process. Finally, a model of a PV inverter is obtained, shown in Fig. 8.
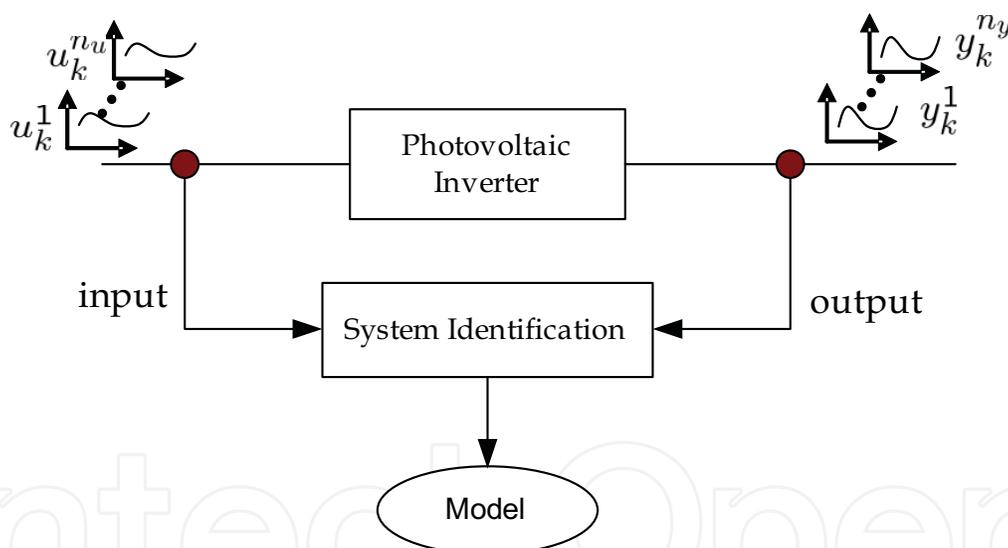

Fig. 8. Experimental design of a photovoltaic inverter modeling using system identification

3.1.5 Model estimation

Data from the system are divided into two groups, i.e., data for estimation (estimate data) and data for validation (validate data). Estimate data are used in the system identification and validate data are used to check and improve the modeling to yield higher accuracy.

3.1.6 Model validation

Model validation is done by comparing experimental data or validates data and modeling data. Errors can then be calculated. In this paper, parameters of system identification are optimized to yield a high accuracy modeling by programming softwares.

3.2 Hammerstein-Wiener (HW) nonlinear model

In this section, a combination of the Wiener model and the Hammerstein model called the Hammerstein-Wiener model is introduced, shown in Fig. 9. In the Wiener model, the front part being a dynamic linear block, representing the system, is cascaded with a static nonlinear block, being a sensor. In the Hammerstein model, the front block is a static nonlinear actuator, in cascading with a dynamic linear block, being the system. This model enables combination of a system, sensors and actuators in one model. The described dynamic system incorporates a static nonlinear input block, a linear output-error model and an output static nonlinear block.
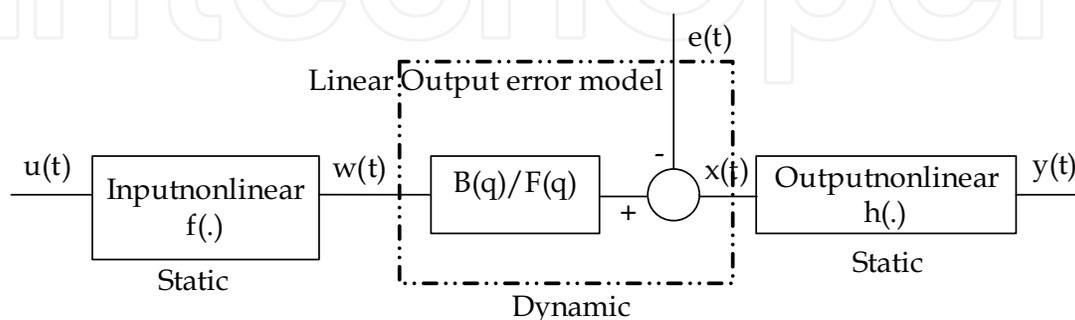

Fig. 9. Structure of Hammerstein-Weiner Model

General equations describing the Hammerstein-Wiener structure are written as the Equation (1)

$$\left.\begin{aligned} w(t) &= f(u(t)) \\ x(t) &= \sum_{i}^{n_u} \frac{B_i(q)}{F_i(q)} w(t - n_k) \\ y(t) &= h(x(t)) \end{aligned}\right\} \tag{1}$$

Which u(t) and y(t) are the inputs and outputs for the system. Where w(t) and x(t) are internal variables that define the input and output of the linear block.

3.2.1 Linear subsystem

The linear block is similar to an output error polynomial model, whose structure is shown in the Equation (2). The number of coefficients in the numerator polynomials B(q) is equal to the number of zeros plus 1, b_n is the number of zeros. The number of coefficients in denominator polynomials F(q) is equal to the number of poles, f_n is the number of poles. The polynomials B and F contain the time-shift operator q, essentially the z-transform which can be expanded as in the Equation (3). n_u is the total number of inputs. n_k is the delay from an input to an output in terms of the number of samples. The order of the model is the sum of b_n and f_n. This should be minimum for the best model.

$$x(t) = \sum_{i}^{n_u} \frac{B_i(q)}{F_i(q)} w(t - n_k) \tag{2}$$

$$\begin{aligned} B(q) &= b_1 + b_2 q^{-1} + \ldots\ldots + b_n q^{-b_n + 1} \\ F(q) &= 1 + f_1 q^{-1} + \ldots\ldots + f_n q^{-f_n} \end{aligned} \tag{3}$$

3.2.2 Nonlinear subsystem

The Hammerstein-Wiener Model composes of input and output nonlinear blocks which contain nonlinear functions f(•) and h(•) that corresponding to the input and output nonlinearities. The both nonlinear blocks are implemented using nonlinearity estimators. Inside nonlinear blocks, simple nonlinear estimators such deadzone or saturation functions are contained.

i. **The dead zone (DZ) function** generates zero output within a specified region, called its dead zone or zero interval which shown in Fig. 10. The lower and upper limits of the dead zone are specified as the start of dead zone and the end of dead zone parameters. Deadzone can define a nonlinear function y = f(x), where f is a function of x, It composes of three intervals as following in the equation (4)

$$\left. \begin{array}{ll} x \leq a & f(x) = x - a \\ a < x < b & f(x) = 0 \\ x \geq b & f(x) = x - b \end{array} \right\} \tag{4}$$

when x has a value between a and b, when an output of the function equal to $F(x) = 0$, this zone is called as a "zero interval".
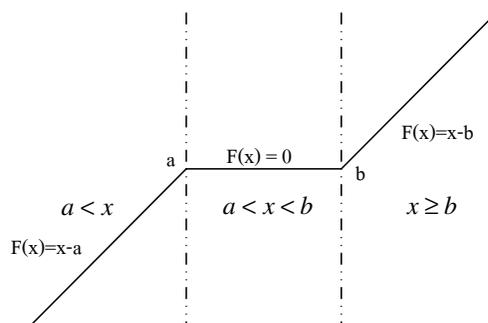

Fig. 10. Deadzone function

ii. **Saturation (ST) function** can define a nonlinear function y = f(x), where *f* is a function of *x*. It composes of three interval as the following characteristics in the equation (5) and Fig. 11. The function is determined between a and b values. This interval is known as a "linear interval"

$$\left. \begin{array}{ll} x > a & f(x) = a \\ a < x < b & f(x) = x \\ x \leq b & f(x) = b \end{array} \right\} \tag{5}$$
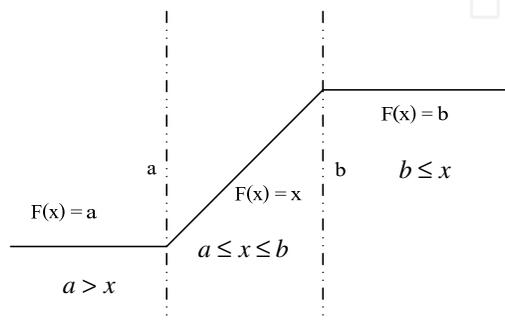

Fig. 11. Saturation function

iii. **Piecewise linear (PW) function** is defined as a nonlinear function, y=f(x) where f is a piecewise-linear (affine) function of x and there are n breakpoints (x_k,y_k) which k=1,...,n. y_k = f(x_k). f is linearly interpolated between the breakpoints. y and x are scalars.

vi. **Sigmoid network (SN) activation function** Both sigmoid and wavelet network estimators which use the neural networks composing an input layer, an output layer and a hidden layer using wavelet and sigmoid activation functions as shown in Fig.12
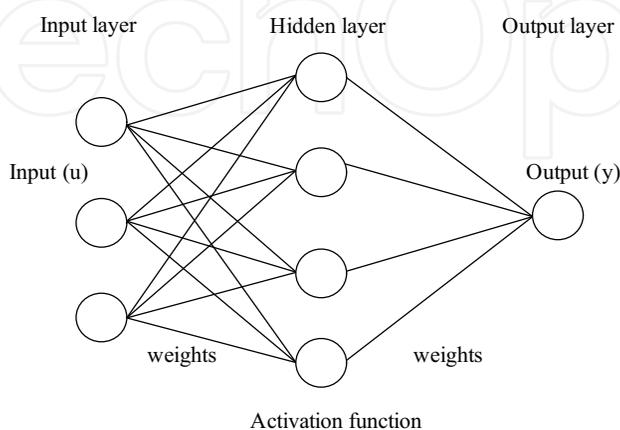

Fig. 12. Structure of nonlinear estimators

A sigmoid network nonlinear estimator combines the radial basis neural network function using a sigmoid as the activation function. This estimator is based on the following expansion:

$$y(u) = (u-r)PL + \sum_{i}^{n} a_i f((u-r)Qb_i - c_i) + d \tag{6}$$

when u is input and y is output. r is the the regressor. Q is a nonlinear subspace and P a linear subspace. L is a linear coefficient. d is an output offset. b is a dilation coefficient., c a translation coefficient and a an output coefficient. f is the sigmoid function, given by the following equation (7)

$$f(z) = \frac{1}{e^{-z} + 1} \tag{7}$$

v. **Wavelet Network (WN) activation function.** The term wavenet is used to describe wavelet networks. A wavenet estimator is a nonlinear function by combination of a wavelet theory and neural networks. Wavelet networks are feed-forward neural networks using wavelet as an activation function, based on the following expansion in the equation (8)

$$y = (u-r)PL + \sum_{i}^{n} as_i * f(bs(u-r)Q + cs) + \sum_{i}^{n} aw_i * g(bw_i(u-r)Q + cw_i) + d \tag{8}$$

Which u and y are input and output functions. Q and P are a nonlinear subspace and a linear subspace. L is a linear coefficient. d is output offset. as and aw are a scaling coefficient and a wavelet coefficient. bs and bw are a scaling dilation coefficient and a

wavelet dilation coefficient. cs and cw are scaling translation and wavelet translation coefficients. The scaling function f (.) and the wavelet function g(.) are both radial functions, and can be written as the equation (9)

$$f(u) = \exp(-0.5 * u' * u)$$
$$g(u) = (\dim(u) - u' * u) * \exp(-0.5 * u' * u)$$
(9)

In a system identification process, the wavelet coefficient (a), the dilation coefficient (b) and the translation coefficient (c) are optimized during model learning steps to obtain the best performance model.

3.3 MIMO Hammerstein-Wiener system identification

The voltage and current are two basic signals considered as input/output of PV grid connected systems. The measured electrical input and output waveforms of a system are collected and transmitted to the system identification process. In Fig. 13 show a PV based inverter system which are considered as SISO (single input-single output) or MIMO (multi input-multi output), depending on the relation of input-output under study [57]. In this paper, the MIMO nonlinear model of power inverters of PV systems is emphasized because this model gives us both voltage and current output prediction simultaneously.
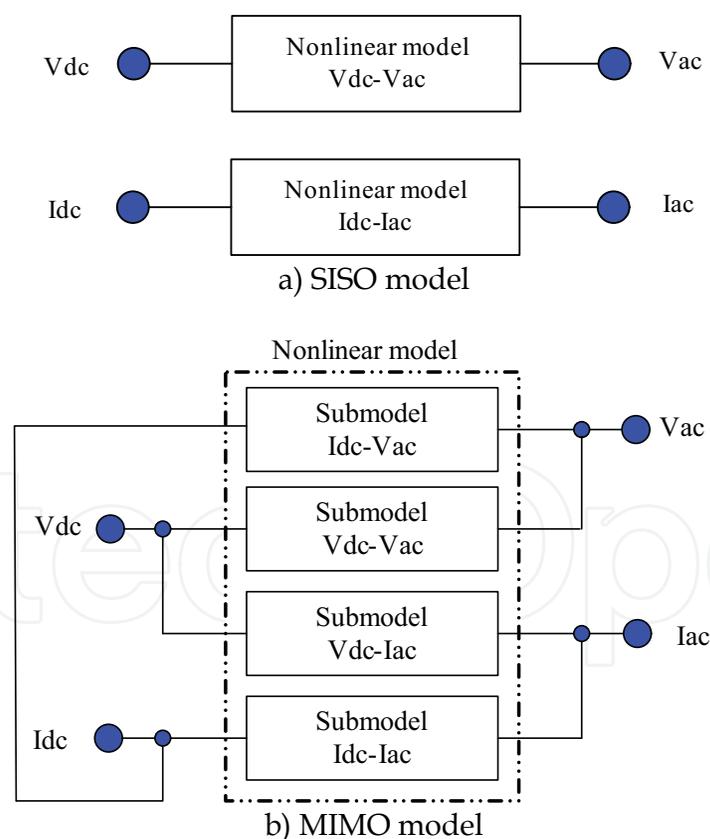

Fig. 13. Block diagram of nonlinear SISO and MIMO inverter model

For one SISO model, there is only one corresponding set of nonlinear estimators for input and output, and one set of linear parameters, i.e. pole b_n, zero f_n and delay n_k, as written in the equation (9). For SIMO, MISO and MIMO models, there would be more than one set of

nonlinear estimators and linear parameters. The relationships between input-output of the MIMO model have been written in the equation (10) whereas v_{dc} is DC voltage, i_{dc} DC current, v_{ac} AC voltage, i_{ac} AC current. q is shift operator as equivalent to z transform. $f(\bullet)$ and $h(\bullet)$ are input and output nonlinear estimators. In this case a deadzone and saturation are selected into the model. In the MIMO model the relation between output and input has four relations as follows (i) DC voltage (v_{dc}) – AC voltage (v_{ac}), (ii) DC voltage (v_{dc}) – AC current (i_{ac}), (iii) DC current (i_{dc}) – AC voltage (v_{ac}) and (iv) DC current(v_{dc})–AC voltage (v_{ac}).

$$\left. \begin{aligned} v_{ac}(t) &= \frac{B(q)}{F(q)} f(v_{dc}(t-n_k)) + e(t) \\ i_{ac}(t) &= \frac{B(q)}{F(q)} f(i_{dc}(t-n_k)) + e(t) \end{aligned} \right\} \tag{10}$$

$$\left. \begin{aligned} V_{ac}(t) &= h\left(\frac{B_1(q)}{F_1(q)} f(v_{dc}(t-n_{k1})) + e(t) \right) \otimes h\left(\frac{B_2(q)}{F_2(q)} f(i_{dc}(t-n_{k2})) + e(t) \right) \\ I_{ac}(t) &= h\left(\frac{B_3(q)}{F_3(q)} f(v_{dc}(t-n_{k3})) + e(t) \right) \otimes h\left(\frac{B_4(q)}{F_4(q)} f(i_{dc}(t-n_{k4})) + e(t) \right) \end{aligned} \right\} \tag{11}$$

$$\begin{aligned} B_i(q) &= b_1 + b_2 + ... + b_{n_{bi}} q^{-n_{bi}+1} \\ F_i(q) &= f_1 + f_2 + ... + f_{n_{fi}} q^{-n_{fi}+1} \end{aligned} \tag{12}$$

Where n_{bi}, n_{fi} and n_{ki} are pole, zero and delay of linear model. Where as number of subscript i are 1,2,3 and 4 which stand for relation between DC voltage-AC voltage, DC current-AC voltage, DC voltage-AC current and DC current-AC current respectively. The output voltage and output current are key components for expanding to the other electrical values of a system such power, harmonic, power factor, etc. The linear parameters, zeros, poles and delays are used to represent properties and relation between the system input and output. There are two important steps to identify a MIMO system. The first step is to obtain experimental data from the MIMO system. According to different types of experimental data, the second step is to select corresponding identification methods and mathematical models to estimate model coefficients from the experimental data. The model is validated until obtaining a suitable model to represent the system. The obtained model provides properties of systems. State-space equations, polynomial equations as well as transfer functions are used to describe linear systems. Nonlinear systems can be describes by the above linear equations, but linearization of the nonlinear systems has to be carried out. Nonlinear estimators explain nonlinear behaviors of nonlinear system. Linear and nonlinear graphical tools are used to describe behaviors of systems regarding controllability, stability and so on.

4. Experimental

In this work, we model one type of a commercial grid connected single phase inverters, rating at 5,000 W. The experimental system setup composes of the inverter, a variable DC power supply (representing DC output from a PV array), real and complex loads, a digital power meter, a digital oscilloscope, , a AC power system and a computer, shown

schematically in Fig 14. The system is connected directly to the domestic electrical system (low voltage). As we consider only domestic loads, we need not isolate our test system from the utility (high voltage) by any transformer. For system identification processes, waveforms are collected by an oscilloscope and transmitted to a computer for batch processing of voltage and current waveforms.
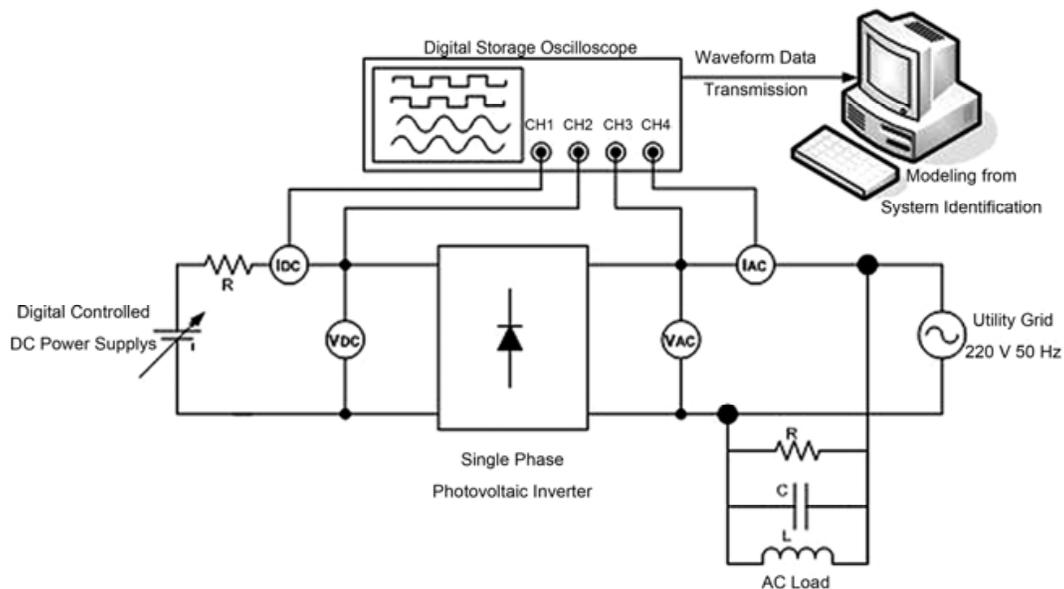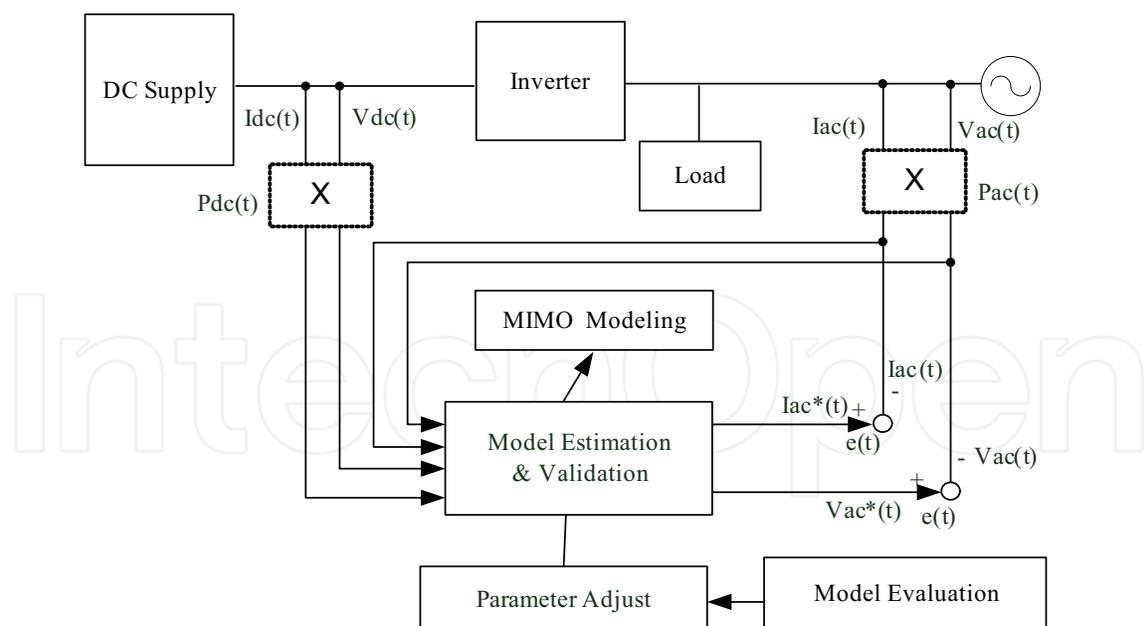

Fig. 14. Experimental setup

Fig. 15. An inverter modeling using system identification process

Major steps in experimentation, analysis and system identifications are composed of Testing scenarios of six steady state conditions and two transient conditions are carried out on the inverter, from collected data from experiments, voltage and current waveform data are divided in two groups to estimate models and to validate models previously mentioned.

The system identification scheme is shown in Fig.15. Good accuracy of models are achieved by selecting model structures and adjusting the model order of linear terms and nonlinear estimators of nonlinear systems. Finally, output voltage and current waveforms for any type of loads and operating conditions are then constructed from the models. This allows us to study power quality as required.

4.1 Steady state conditions

To emulate working conditions of PVGCS systems under environment changes (irradiance and temperature) affecting voltage and current inputs of inverters, six conditions of DC voltage variations and DC current variations. The six conditions are listed as Table 1. They are 3 conditions of a fixed DC current with DC low, medium and high voltage, i.e. , FCLV (Fixed Current Low Voltage), FCMV (Fixed Current Medium Voltage) and FCHV (Fixed Current High Voltage) which shown in Fig. 16. The other three corresponding conditions are a DC fixed voltage with DC low, medium and high current, i.e., FVLC (Fixed Voltage Low Current), FVMC (Fixed Voltage Medium Current), and FVHC (Fixed Voltage High Current) as shown in Fig.17.
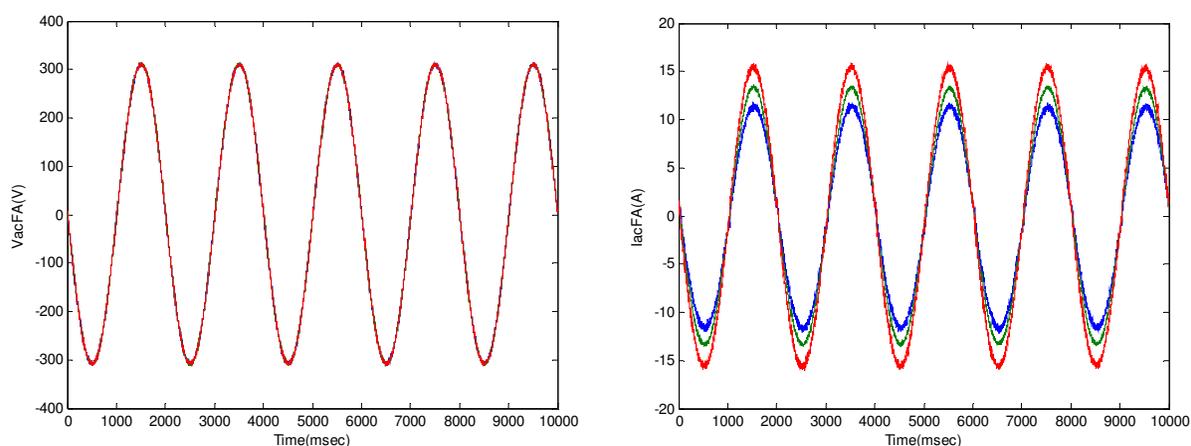

Fig. 16. AC voltage and current waveforms corresponding to FCLV, FCMV and FCHV conditions
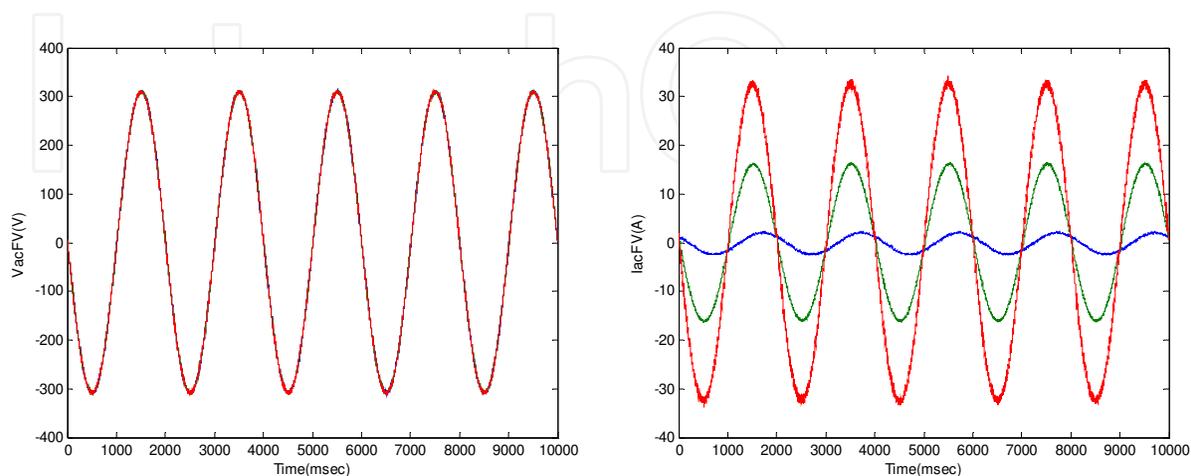

Fig. 17. AC voltage and current waveforms corresponding to FVLC, FVMC and FVHC conditions

No.	Case	Idc (A)	Vdc (V)	Pdc (W)	Iac (A)	Vac (A)	Pac (VA)
1	FCLV	12	210	2520	11	220	2420
2	FCMV	12	240	2880	13	220	2860
3	FCHV	12	280	3360	15	220	3300
4	FVLC	2	235	470	2	220	440
5	FVMC	10	240	2,400	10	220	2,200
6	FVHC	21	245	5,145	23	220	5,060

Table 1. DC and AC parameters of an inverter under changing operating conditions

4.2 Transient conditions

Transient conditions are studied under two cases which composed of step up power transient and step down power transient. The step up condition is done by increasing power output from 440 to1,540 W, and the step down condition from 1,540 to 440 W, shown in Table 2. Power waveform data of the two conditions are divided in two groups, the first group is used to estimate model, the second group to validate model. Examples of captured voltage and current waveforms under the step-up power transient condition (440 W or 2 A) to 1540 W or 7A) and the step-down power transient condition (1540 W or 7A) to 440 W (2A) are shown in Fig. 18 and 19, respectively.
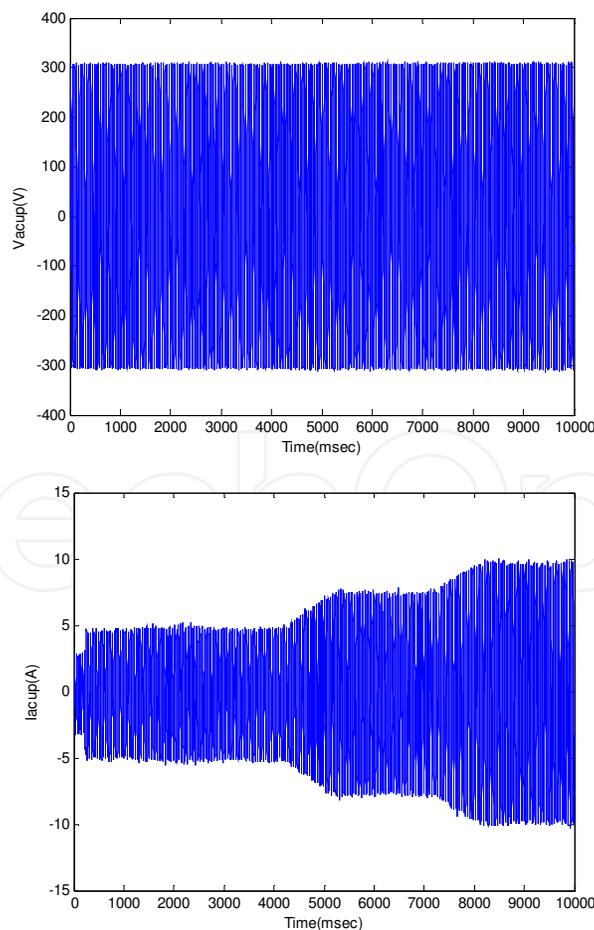

Fig. 18. AC voltage and current waveforms under the step up transient condition
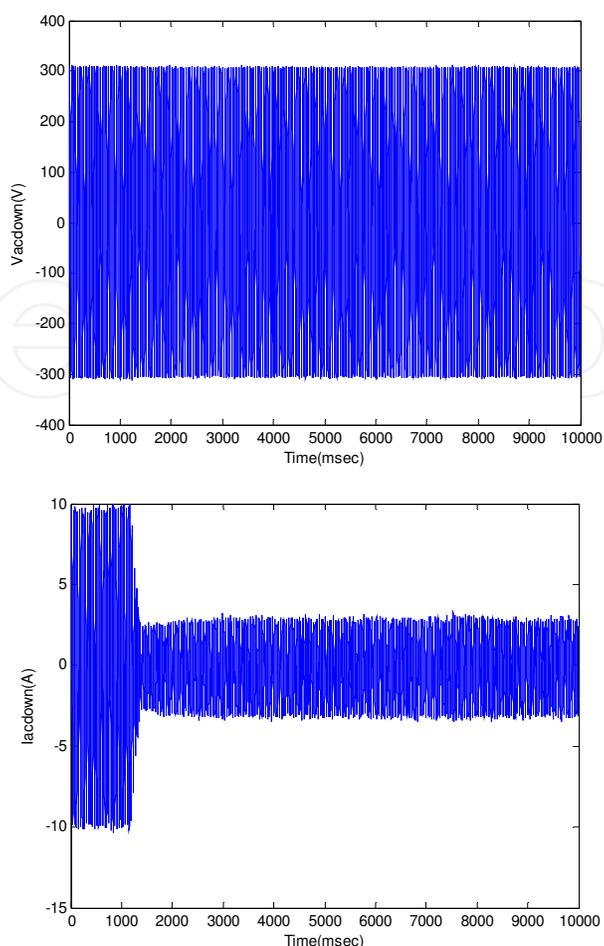
Fig. 19. AC voltage and current waveforms under the step down transient condition

Electrical parameters	Voltage, current and power for transient step down conditions		Voltage, current and power for transient step up conditions	
AC output voltage (V)	220	220	220	220
AC output current (A)	7	2	2	7
AC output power (W)	1540	440	440	1540

Table 2. Inverter operations under step up/down conditions

5. Results and discussion

In the next step, data waveforms are divided into the "estimate data set" and the "validate data set". Examples are shown in Fig. 20, whereby the first part of the AC and DC voltage waveforms are used as the estimate data set and the second part the validate data set. The system identification process is executed according to mentioned descriptions on the Hammerstein-Wiener modeling.

The validation of models is taken by considering (i) model order by adjusting the number of poles plus zeros. The system must have the lowest-order model that adequately captures the system dynamics.(ii) the best fit, comparing between modeling and experimental outputs, (iii) FPE and AIC, both of these values need be lowest for high accuracy of modeling (iv)

Nonlinear behavior characteristics. For example, linear interval of saturation, zero interval of dead-zone, wavenet, sigmoid network requiring the simplest and less complex function to explain the system. Model properties, estimators, percentage of accuracy, final Prediction Error-FPE and Akaikae Information Criterion-AIC are as follows [58]:
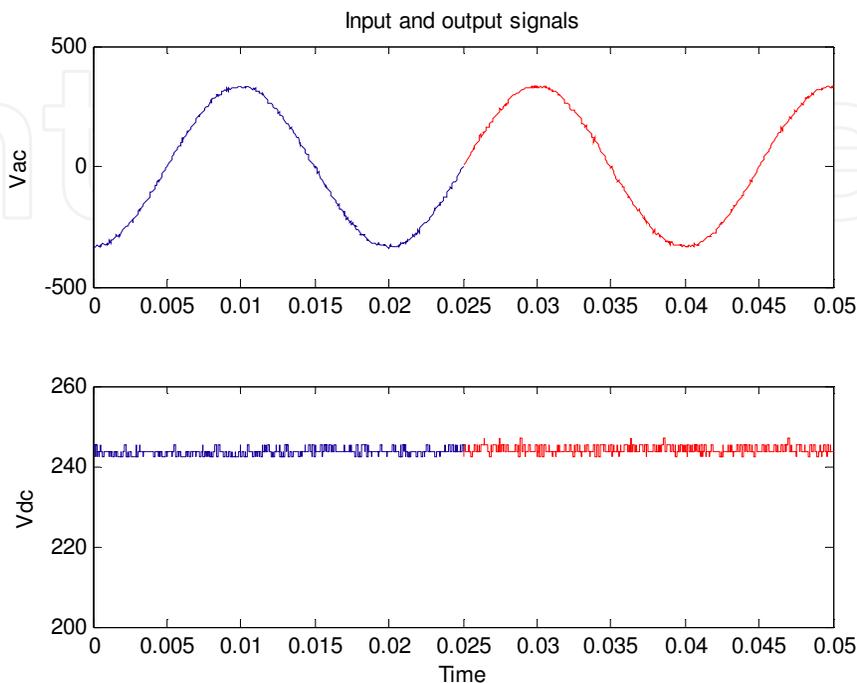

Fig. 20. Data divided into Estimated and validated data

Criteria for Model selection

The percentage of the best fit accuracy in equation (13) is obtained from comparison between experimental waveform and simulation modeling waveform.

$$Best\ fit = 100 * (1 - norm(y^* - y) / norm(y - \bar{y})) \tag{13}$$

where y* is the simulated output, y is the measured output and $\bar{y}$ is the mean of output. FPE is the Akaike Final Prediction Error for the estimated model, of which the error calculation is defined as equation (14)

$$FPE = V\left(\frac{1 + d/N}{1 - d/N}\right) \tag{14}$$

where V is the loss function, d is the number of estimated parameters, N is the number of estimation data. The loss function V is defined in Equation (15) where θ_N represents the estimated parameters.

$$V = \det\left(\frac{1}{N}\sum_1^N \varepsilon(t,\theta_N)\left(\varepsilon(t,\theta_N)\right)^T\right) \tag{15}$$

The Final Prediction Error (FPE) provides a measure of a model quality by simulating situations where the model is tested on a different data set. The Akaike Information

Criterion (AIC), as shown in equation (16), is used to calculate a comparison of models with different structures.

$$AIC = \log V + \frac{2d}{N} \qquad (16)$$

Waveforms of input and output from the experimental setup consist of DC voltage, DC output current, AC voltage and AC output current. Model properties, estimators, percentage of accuracy, Final Prediction Error - FPE and Akaikae Information Criterion - AIC of the model are shown in Table 3. Examples of voltage and current output waveforms of multi input-multi output (MIMO) model in steady state condition (FVMC) having accuracy 97.03% and 91.7 % are shown in Fig 21.

Type	I/P	O/P	Linear model parameters [nb$_1$ nb$_2$ nb$_3$ nb$_4$] poles [nf$_1$ nf$_2$ nf$_3$ nf$_4$] zeros [nk$_1$ nk$_2$ nk$_3$ nk$_4$] delays	% fit Voltage Current	FPE	AIC
Steady state conditions						
FCLV	DZ	DZ	[4 4 3 5]; [5 5 3 6]; [3 4 4 2]	87.3 85.7	3,080.90	10.9
FCMV	PW	PW	[5 2 4 4]; [4 2 3 4]; [2 2 4 3];	84.5 86.4	729.03	6.59
FCHV	ST	ST	[2 2 3 4]; [1 2 1 2]; [2 1 3 2];	89.5 88.7	26.27	3.26
FVLC	SN	SN	[3 6 3 2]; [8 5 4 3]; [2 4 3 5];	56.8 60.5	0.07	2.57
FVMC	WN	WN	[3 4 2 5]; [4 2 3 4]; [2 3 2 4];	97.03 91.7	254.45	7.89
FVHC	WN	WN	[1 4 3 5]; [5 2 3 5]; [1 3 2 4];	88 94	3,079.8	10.33
Transient conditions						
Step Up	DZ	DZ	[3 4 2 4]; [4 5 4 3]; [2 3 5 5]; [4 5 2 2];	91.75 87.20	3,230	7.40
Step Down	PW	PW	[3 5 5 3]; [3 5 4 3]; [3 5 5 4]; [4 4 4 1];	85.99 85.12	3,233	10.0

Table 3. Results of a PV inverter modeling using a Hammerstein-Wiener model
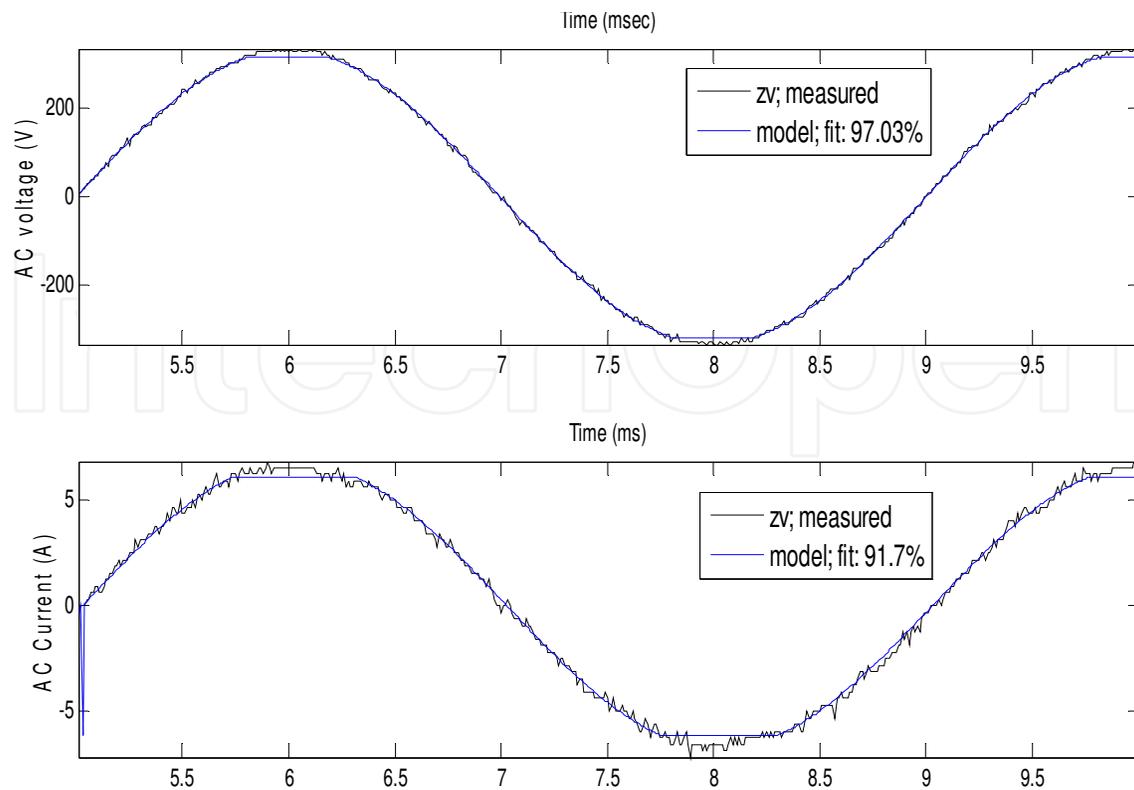
Fig. 21. Comparison of AC voltage and current output waveforms of a steady state FVMC MIMO model

In Table 3 n_{bi}, n_{fi} and n_{ki} are poles, zeros and delays of a linear model. The subscript (1, 2, 3 and 4) stands for relations between DC voltage-AC voltage, DC current-AC voltage, DC voltage-AC current and DC current-AC current respectively. Therefore, the linear parameters of the model are $[n_{b1},n_{b2},n_{b3},n_{b4}]$, $[n_{f1},n_{f2},n_{f3},n_{f4}]$, $[n_{k1},n_{k2},n_{k3},n_{k4}]$.

The first value of percentages of fit in each type, shown in the Table 3, is the accuracy of the voltage output, the second the current output from the model. From the results, nonlinear estimators can describe the photovoltaic grid connected system. The estimators are good in terms of accuracy, with a low order model or a low FPE and AIC. Under most of testing conditions, high accuracy of more than 85% is achieved, except the case of FVLC. This is because of under such an operating condition, the inverter has very small current, and it is operating under highly nonlinear behavior. Then complex of nonlinear function and parameter adjusted is need for achieve the high accuracy and low order of model. After obtaining the appropriate model, the PVGCS system can be analyzed by nonlinear and linear analyses. Nonlinear parts are analyzed from the properties of nonlinear function such as dead-zone interval, saturation interval, piecewise range, Sigmoid and Wavelet properties. Nonlinear properties are also considered, e.g. stability and irreversibility In order to use linear analysis, Linearization of a nonlinear model is required for linear control design and analysis, with acceptable representation of the input/output behaviors. After linearizing the model, we can use control system theory to design a controller and perform linear analysis. The linearized command for computing a first-order Taylor series approximation for a system requires specification of an operating point. Subsequently, mathematical representation can be obtained, for example, a discrete time invariant state space model, a transfer function and graphical tools.

6. Applications: Power quality problem analysis

A power quality analysis from the model follows the Standard IEEE 1159 Recommend Practice for Monitoring Electric Power Quality [59]. In this Standard, the definition of power quality problem is defined. In summary, a procedure of this Standard when applied to operating systems can be divided into 3 stages (i) Measurement Transducer, (ii) Measurement Unit and (iii) Evaluation Unit. In comparing operating systems and modeling, modeling is more advantageous because of its predictive power, requiring no actual monitoring. Based on proposed modeling, the measurement part is replaced by model prediction outputs, electrical values such as RMS and peak values, frequency and power are calculated, rather than measured. The actual evaluation is replaced by power quality analysis. The concept representation is shown in Fig.22.
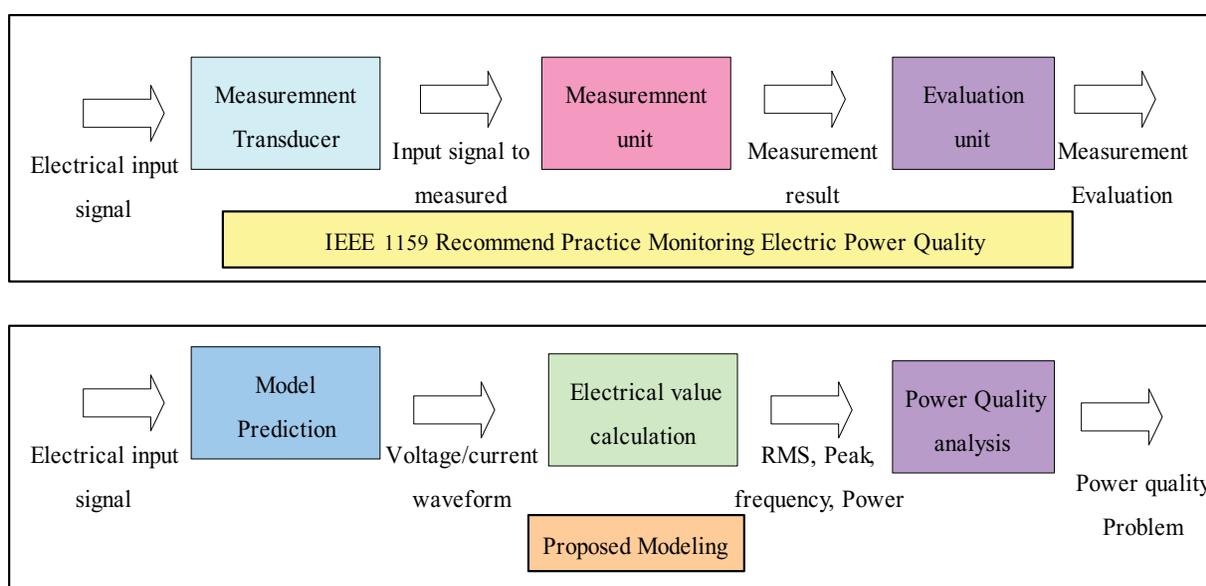
Fig. 22. Diagram of power quality analysis from IEEE 1159 and application to modeling

6.1 Model output prediction

In this stage, the model output prediction is demonstrated. From the 8 operation conditions selected in experimental, we choose two representative case. One is the steady state Fix Voltage High Current (FVHC) condition, the other the transient step down condition. To illustrate model predictive power, Fig.23 shows an actual and predictive output current waveforms of the transient step down condition. We see good agreement between experimental results and modeling results.

6.2 Electrical parameter calculation

In this stage, output waveforms are used to calculate RMS, peak and per unit (p.u.) values, period, frequency, phase angle, power factor, complex power (real, reactive and apparent power) Total Harmonic Distortion - THD.

6.2.1 Root mean square

RMS values of voltage and current can be calculated from the following equations:

$$V_{rms} = \sqrt{\frac{1}{T}\int_0^T v^2(t)dt}$$

$$I_{rms} = \sqrt{\frac{1}{T}\int_0^T v^2(t)dt}$$

(17)

$$V_m = \sqrt{2}V_{rms}$$

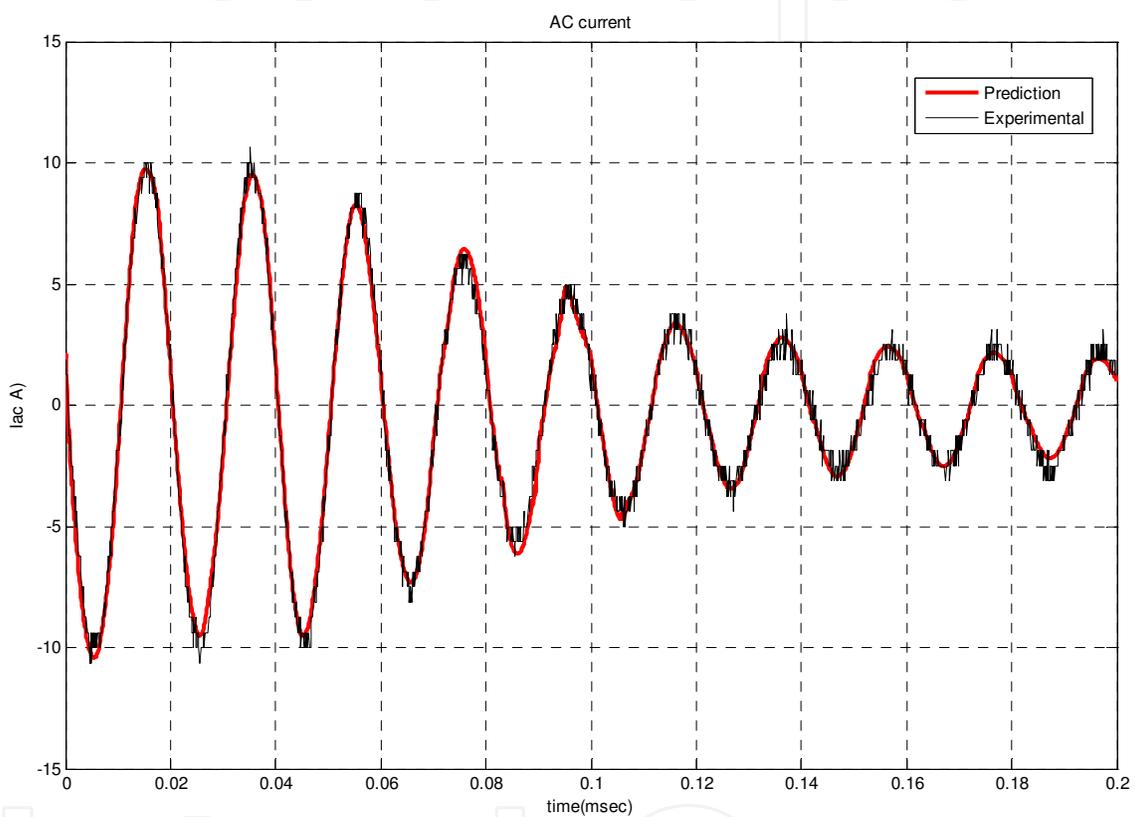$$I_m = \sqrt{2}I_{rms}$$

(18)

Fig. 23. Prediction and experiment results of AC output current under a transient step down condition

6.2.2 Period, frequency and phase angle

We calculate a phase shift between voltage and current from the equation (19), and the frequency (f) from equation (20).

$$\phi = \frac{\Delta t(ms) \cdot 360°}{T\ ms}$$

(19)

$$f = \frac{1}{T}$$

(20)

Δt is time lagging or leading between voltage and current (ms), T is the waveform period.

6.2.3 Power factor, apparent power, active power and reactive power

The power factor, the apparent power S (VA), the active power P (W), and the reactive power Q (Var) are related through the equations

$$PF = \cos\phi = \frac{P(W)}{S(VA)} \tag{21}$$

$$S = VI' \tag{22}$$

$$P = S\cos\phi \tag{23}$$

$$Q = S\sin\phi \tag{24}$$

6.2.4 Harmonic calculation

Total harmonic distortion of voltage (THD$_v$) and current (THD$_i$) can be calculated by the Equations 25 and 26, respectively.

$$\%THD_i = \frac{\sqrt{\sum_{h=2}^{\infty} I_{h(rms)}^2}}{I_{1(rms)}} x\ 100\% \tag{25}$$

$$\%THD_v = \frac{\sqrt{\sum_{h=2}^{\infty} V_{h(rms)}^2}}{V_{1(rms)}} x\ 100\% \tag{26}$$

Where Vh (rms) is RMS value of h th voltage harmonic , Ih (rms) RMS value of h th current harmonic,   V1 (rms) RMS value of fundamental voltage and I1 (rms)   RMS value of fundamental current

Parameter	Steady state FVHC condition			Transient step down condition		
	Experimental	Modeling	% Error	Experimental	Modeling	% Error
Vrms (V)	218.31	218.04	0.12	217.64	218.20	-0.26
Irms (A)	23.10	23.21	-0.48	4.47	4.45	0.45
Frequency (Hz)	50	50	0.00	50.00	50.00	0.00
Power Factor	0.99	0.99	0.00	0.99	0.99	0.00
THDv (%)	1.15	1.2	-4.35	1.18	1.24	-5.08
THDi (%)	3.25	3.12	4.00	3.53	3.68	-4.25
S (VA)	5044.38	5060.7	-0.32	972.85	970.99	0.19
P (W)	4993.94	5010.1	-0.32	963.12	961.28	0.19
Q (Var)	711.59	713.85	-0.32	137.24	136.97	0.19
V p.u.	0.99	0.99	0.00	0.98	0.99	-1.02

Table 4. Comparison of measured and modeled electrical parameters of the FVHC condition and the transient step down condition

We next demonstrate accuracy and precision of power quality prediction from modeling. Table 4 shows the comparisons. Two representative cases mentioned above are given, i.e. the steady state Fix Voltage High Current (FVHC) condition, and the transient step down condition. Comparison of THDs is shown in Fig. 23. Agreements between experiments and modeling results are good.
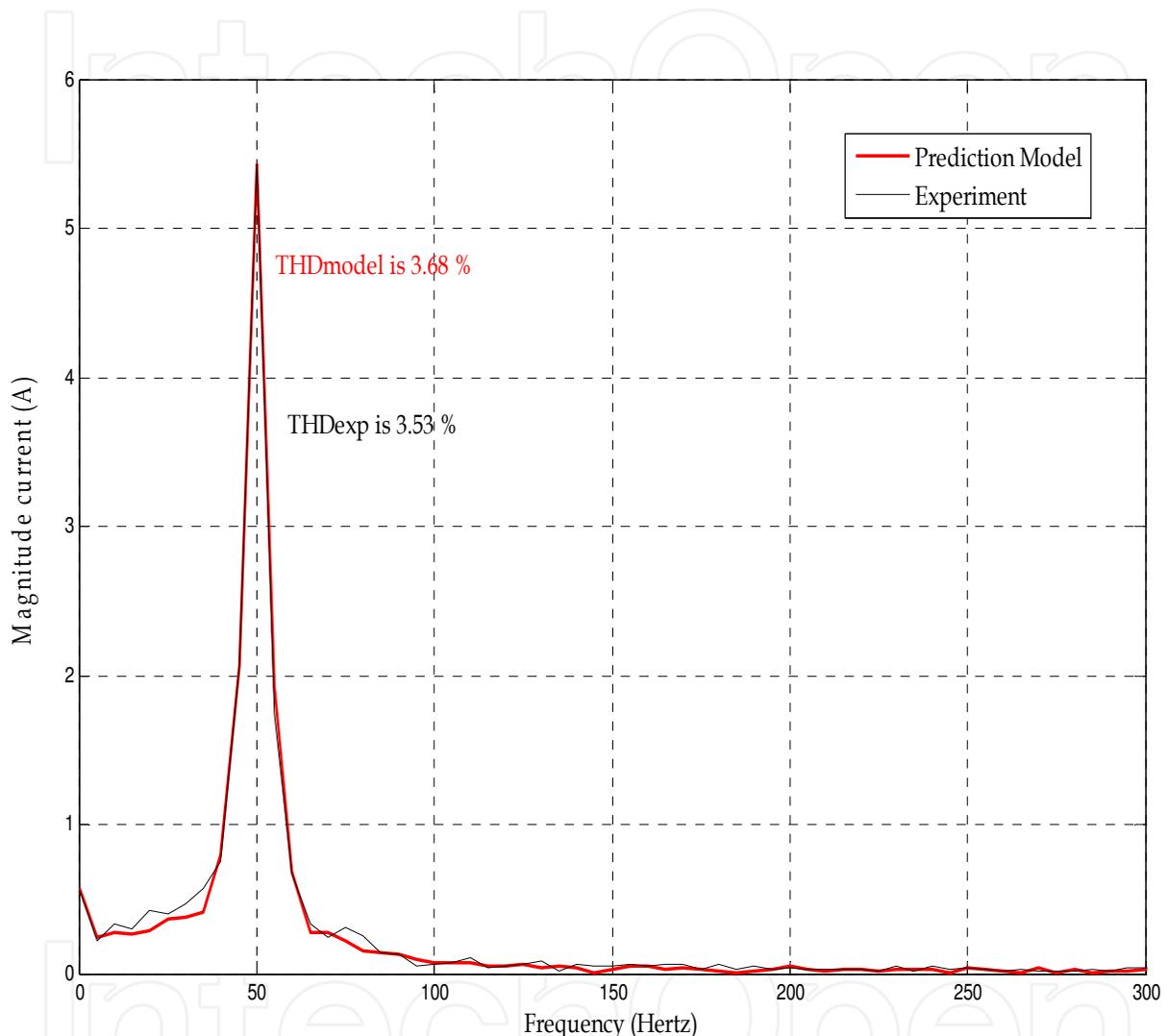

Fig. 24. Comparison of measured and modeled THD of AC current of the transient step down condition

6.3 Power quality problem analysis

The power quality phenomena are classified in terms of typical duration, typical voltage magnitude and typical spectral content. They can be broken down into 7 groups on transient, short duration voltage, long duration voltage, voltage unbalance, waveform distortion, voltage fluctuation or flicker, frequency variation. Comparisons of the Standard values and modeled outputs of the FVHC and the transient step down conditions are shown in Table 5. The results show that under both the steady state and the transient cases, good power quality is achieved from the PVGCS.

Type	Typical Duration	Typical Voltage Magnitude	Typical Spectral Content	Steady State FVHC	Transient Step down	Result
1.Transient - Impulsive - Oscillation - low frequency - medium frequency - high frequency	5 ns – 0.1ms 0.3-50 ms 5-20 ms 0-5 ms	 0.4 pu. 0-8 pu. 0.4 pu.	 < 5 kHz 5-500 kHz 0.5–5 MHz	0.99 pu.	0.99 pu.	Pass
2.Short Duration - voltage sag - voltage swell	10 ms-1 min 10 ms-1 min	0.1-0.9 pu. 1.1-1.8 pu.	-	0.99 pu.	0.99 pu.	Pass
3. Long Duration - overvoltage (OV) - undervoltage (UV) - voltage Interruption	> 1 min > 1 min > 1 min	> 1.1 pu. < 0.9 pu. 0 pu.	 -	0.99 pu.	0.99 pu.	Pass
4. Voltage Unbalance	Steady state	0.5-2%	-	-	-	-
5.Waveform distortion - Harmonic voltage - Harmonic Current - Interharmonic - DC offset - Notching - Noise	 Steady state Steady state Steady state Steady state Steady state Steady state	 < 5% THD < 20% THD 0-2% 0-0.1% - 0-1%	 0-100th 0-100th 0-6 kHz < 200 kHz - Broad band	 1.20 % 3.25 % - - - -	 1.24 % 3.68 % - - - -	 Pass Pass - - - -
6.Voltage fluctuation - Flicker	 Intermittent	 0.1-7%	 < 25 Hz	 0.01%	 0.01%	 Pass
7.Frequency variation - Overfrequency - Underfrequency	 < 10 s	 -	± 3 Hz > 53 Hz < 47 Hz	 50	 50	 Pass

Table 5. Comparison modeling output with Categories and Typical Characteristics of power system electromagnetic phenomena

7. Conclusions

In this paper, a PVGCS system is modeled by the Hammerstein-Wiener nonlinear system identification method. Two main steps to obtain models from a system identification process are implemented. The first step is to set up experiments to obtain waveforms of DC inverter voltage/current, AC inverter voltage/current, point of common coupling (PCC) voltage, and grid and load current. Experiments are conducted under steady state and transient conditions for commercial rooftop inverters with rating of few kW, covering resistive and complex loads. In the steady state experiment, six conditions are carried out. In the transient case, two conditions of operating conditions are conducted. The second stage is to derive system models from system identification software. Collected waveforms are transmitted

into a computer for data processing. Waveforms data are divided in two groups. One group is used to estimate models whereas the other group to validate models. The developed programming determines various model waveforms and search for model waveforms of maximum accuracy compared with actual waveforms. This is achieved through selecting model structures and adjusting the model order of the linear terms and nonlinear estimators of nonlinear terms. The criteria for selection of a suitable model are the "Best Fits" as defined by the software, and a model order which should be minimum.

After obtaining appropriate models, analysis and prediction of power quality are carried out. Modeled output waveforms relating to power quality analysis are determined from different scenarios. For example, irradiances and ambient temperature affecting DC PV outputs and nature of complex local load can be varied. From the model output waveforms, determination is made on power quality aspects such as voltage level, total harmonic distortion, complex power, power factor, power penetration and frequency deviation. Finally, power quality problems are classified.

Such modelling techniques can be used for system planning, prevention of system failures and improvement of power quality of roof-top grid connected systems. Furthermore, they are not limited to PVGCS but also applicable to other distributed energy generators connected to grids.

8. Acknowledgements

9. References

[1] Bollen M. H. J. and Hager M., Power quality: integrations between distributed energy resources, the grid, and other customers. Electrical Power Quality and Utilization Magazine, vol. 1, no. 1, pp. 51–61, 2005.

[2] Vu Van T., Belmans R., Distributed generation overview: current status and challenges. Inter-national Review of Electrical Engineering (IREE), vol. 1, no. 1, pp. 178–189, 2006.

[3] Pedro González, "Impact of Grid connected Photovoltaic System in the Power Quality of a Network", Power Electrical and Electronic Systems (PE&ES), School of Industrial Engineering, University of Extremadura.

[4] Barker P. P., De Mello R. W., Determining the impact of distributed generation on power systems: Part 1 – Radial distribution systems. PES Summer Meeting, IEEE, Vol. 3, pp. 1645–1656, 2000.

[5] Vu Van T., Impact of distributed generation on power system operation and control. PhD Thesis, Katholieke Universiteit Leuven, 2006.

[6] Muh. Imran Hamid and Makbul Anwari, "Single phase Photovoltaic Inverter Operation Characteristic in Distributed Generation System", Distributed Generation, Intech book, 2010

[7] Vu Van T., Driesen J., Belmans R., Interconnection of distributed generators and their influences on power system. International Energy Journal, vol. 6, no. 1, part 3, pp. 127–140, 2005.

[8] A. Moreno-Munoz, J.J.G. de-la-Rosa, M.A. Lopez-Rodriguez, J.M. Flores-Arias, F.J. Bellido-Outerino, M. Ruiz-de-Adana, "Improvement of power quality using distributed generation", Electrical Power and Energy Systems 32 (2010) 1069–1076

[9] P.R.Khatri, V.S.Jape, N.M.Lokhande, B.S.Motling, "Improving Power Quality by Distributed Generation" Power Engineering Conference, 2005. IPEC 2005. The 7th International.

[10] Vu Van T., Driesen J., Belmans R., Power quality and voltage stability of distribution system with distributed energy resources. International Journal of Distributed Energy Resources, vol. 1, no. 3, pp. 227–240, 2005.

[11] Woyte A., Vu Van T., Belmans R., Nijs J., Voltage fluctuations on distribution level introduced by photovoltaic systems. IEEE Transactions on Energy Conversion, vol. 21, no. 1, pp. 202–209, 2006.

[12] Thongpron, K.Kirtara, Effects of low radiation on the power quality of a distributed PV-grid connected system, Solar Energy Materials and Solar Cells Solar Energy Materials and Solar Cells, Vol. 90, No. 15. (22 September 2006), pp. 2501-2508.

[13] S.K. Khadem, M.Basu and M.F.Conlon, "Power quality in Grid connected Renewable Energy Systems : Role of Custom Power Devices", International conference on Renewable Energies and Power quality (ICREPQ'10), Granada, Spain, 23rd to 25th March, 2010

[14] Mohamed A. Eltawil Zhengming Zhao, "Grid-connected photovoltaic power systems: Technical and potential problems—A review" Renewable and Sustainable Energy Reviews Volume 14, Issue 1, January 2010, Pages 112-129

[15] Soeren Baekhoej Kjaer, et al., "A Review of Single-Phase Grid-Connected inverters for Photovoltaic Modules, EEE Transactions and industry applications, Transactions on Industry Applications, Vol. 41, No. 5, September 2005

[16] F. Blaabjerg, Z. Chen and S. B. Kjaer, "Power Electronics as Efficient Interface in Dispersed Power Generation Systems." IEEE Trans. on Power Electronics 2004; vol.19 no. 5. Pp. 1184-1194. 2000.

[17] Chi, Kong Tse, "Complex behavior of switching power converters", Boca Raton : CRC Press, c2004

[18] Giraud, F., Steady-state performance of a grid-connected rooftop hybrid wind-photovoltaic power system with battery storage, IEEE Transactions on Energy Conversion, 2001.

[19] G.Saccomando, J.Svensson, "Transient Operation of Grid-connected Voltage Source Converter Under Unbalanced Voltage Conditions", IEEE Industry Applications Conference, 2001.

[20] Li Wang and Ying-Hao Lin, "Small-Signal Stability and Transient Analysis of an Autonomous PV System", Transmission and Distribution Conference and Exposition, 2008.

[21] Zheng Shi-cheng, Liu Xiao-li, Ge Lu-sheng; , "Study on Photovoltaic Generation System and Its Islanding Effect," Industrial Electronics and Applications, 2007. ICIEA 2007. 2nd IEEE Conference on , 23-25 May 2007, pp.2328-2332

[22] Pu kar Mahat, et al, "Review of Islanding Detection Methods for Distributed Generation", DRPT 6-9 April 2008, Nanjing, China.

[23] Yamashita, H. et al. "A novel simulation technique of the PV generation system using real weather conditions Proceedings of the Power Conversion Conference, 2002 PCC Osaka 2002.

[24] Golovanov, N, "Steady state disturbance analysis in PV systems", IEEE Power Engineering Society General Meeting, 2004.

[25] D. Maksimovic , et al, "Modeling and simulation of power electronic converters," Proc. IEEE, vol. 89, pp. 898, Jun. 2001

[26] R. D. Middlebrook and S. Cuk "A general unified approach to modeling switching converter power stages," Int.J. Electron., vol. 42, pp. 521, Jun. 1977.

[27] Marisol Delgado and Hebertt Sira-RamírezA bond graph approach to the modeling and simulation of switch regulated DC-to-DC power supplies, Simulation Practice and Theory Volume 6, Issue 7, 15 November 1998, Pages 631-646.

[28] R.E. Araujo, et al, "Modelling and simulation of power electronic systems using a bond formalism", Proceeding of the 10th Mediterranean Conference on control and Automation – MED2002, Lisbon, Portugal, July 9-12 2002.

[29] H. I. Cho, "A Steady-State Model of the Photovoltaic System in EMTP", The International Conference on Power Systems Transients (IPST2009), Kyoto, Japan June 3-6, 2009

[30] Y. Jung, J. Sol, G. Yu, J. Choj, "Modelling and analysis of active islanding detection methods for photovoltaic power conditioning systems," Electrical and Computer Engineering, 2004. Canadian Conference on , vol.2, 2-5 May 2004, pp. 979- 982.

[31] Seul-Ki Kim,"Modeling and simulation of a grid-connected PV generation system for electromagnetic transient analysis", Solar Energy, Volume 83, Issue 5, May 2009, Pages 664-678.

[32] Onbilgin, Guven, et al, "Modeling of power electronics circuits using wavelet theory", Sampling Theory in Signal and Image Processing, September, 2007.

[33] George A. Bekey, "System identification- an introduction and a survey, Simulation, Transaction of the society for modeling and simulation international", October 1970 vol. 15 no. 4, 151-166.

[34] J.sjoberg, et al., "Nonlinear black-box Modeling in system identification: a unified overview, Automatica Journal of IFAC, Vol 31, Issue 12, December 1995.

[35] K. T. Chau and C. C. Chan "Nonlinear identification of power electronics systems," Proc. Int. Conf. Power Electronics and D20ve Systems, vol. 1, 1995, p. 329.

[36] J. Y. Choi , et al. "System identification of power converters based on a black-box approach," IEEE Trans. Circuits Syst. I, Fundam. Theory Appl., vol. 45, pp. 1148, Nov. 1998.

[37] F.O. Resende and J.A.Pecas Lopes, "Development of Dynamic Equivalents for Microgrids using system identification theory", IEEE of Power Technology, Lausanne, pp. 1033-1038, 1-5 July 2007.

[38] N.Patcharaprakiti, et al, "Modeling of Single Phase Inverter of Photovoltaic System Using System Identification", Computer and Network Technology (ICCNT), 2010 , April 2010, Page(s): 462 – 466.

[39] Hatanaka, et al. , "Block oriented nonlinear model identification by evolutionary computation approach", Proceedings of IEEE Conference on Control Applications, 2003, Vol 1, pp 43- 48, June 2003.

[40] Li, G. Identification of a Class of Nonlinear Autoregressive Models With Exogenous Inputs Based on Kernel Machines, IEEE Transactions on Signal Processing, Vol 59, Issue 5, May 2011.

[41] T. Wigren, "User choices and model validation in system identification using nonlinear Wiener models", Proc13:th IFAC Symposium on System Identification, Rotterdam, The Netherlands, pp. 863-868, August 27-29, 2003.

[42] Alonge, et al, "Nonlinear Modeling of DC/DC Converters Using the Hammerstein's Approach" IEEE Transactions on Power Electronics, July 2007, Volume: 22, Issue: 4,pp. 1210-1221.

[43] Guo. F. and Bretthauer, G. "Identification of cascade Wiener and Hammerstein systems", In Proceeding. of ISATED Conference on Applied Simulation and Modeling, Marbella, Spain, September, 2003.

[44] N.Patcharaprakiti and et al., "Modeling of single phase inverter of photovoltaic system using Hammerstein–Wiener nonlinear system identification", Current Applied Physics 10 (2010) S532–S536,

[45] A Guide To Photovoltaic Panels, PV Panels and Manufactures' Data, January 2009.

[46] Tomas Markvart, "Solar electricity", Wiley, 2000

[47] D.R.Myers, "Solar Radiation Modeling and Measurements for Renewable Energy Applications: Data and Model Quality", International Expert Conference on Mathematical Modeling of Solar Radiation and Daylight—Challenges for the 21st, Century, Edinburgh, Scotland

[48] R.H.B. Exell, "The fluctuation of solar radiation in Thailand", Solar Energy, Volume 18, Issue 6, 1976, Pages 549-554.

[49] M. Calais, J. Myrzik, T. Spooner, V.G. Agelidis, "Inverters for Single-phase Grid Connected Photovoltaic Systems - An Overview," Proc. IEEE PESC'02, vol. 2. 2002. Pp 1995-2000.

[50] Photong, C. and et al, "Evaluation of single-stage power converte topologies for grid-connected Photovoltaic", IEEE International Conference on Industrial Technology (ICIT), 2010.

[51] Y. Xue, L.Chang, S. B. Kj r, J. Bordonau, and T. Shimizu, "Topologies of Single- Phase Inverters for Small Distributed Power Generators: An Overview," IEEE Trans. on Power Electronics, vol. 19, no. 5, pp. 1305-1314, 2004.

[52] S.H. Ko, S.R. Lee, and H. Dehbonei, "Application of Voltage- and Current- Controlled Voltage Source Inverters for Distributed Generation System," IEEE Trans. Energy Conversion, vol. 21, no.3, pp. 782-792, 2006.

[53] Yunus H.I. and et al., Comparison of VSI and CSI topologies for single-phase active power filters, Power Electronics Specialists Conference, 1996. PESC '96 Record., 27th Annual IEEE

[54] N. Chayawatto, K. Kirtikara, V. Monyakul, C Jivacate, D Chenvidhya, "DC–AC switching converter mode lings of a PV grid-connected system under islanding phenomena", Renewable Energy 34 (2009) 2536–2544.

[55] Lennart Ljung, "System identification : theory for the user", Upper Saddle River, NJ, Prentice Hall PTR, 1999.

[56] Nelles, Oliver, Nonlinear system identification : from classical approaches to neural networks and fuzzy models, 2001

[57] N.Patcharaprakiti and et al., "Nonlinear System Identification of power inverter for grid connected Photovoltaic System based on MIMO black box modeling", GMSTECH 2010 : International Conference for a Sustainable Greater Mekong Subregion, 26-27 August 2010, Bangkok, Thailand.

[58] Lennart Ljung, System Identification Toolbox User Guide, 2009

[59] IEEE 1159, 2009 Recommended practice for monitoring electric power quality.
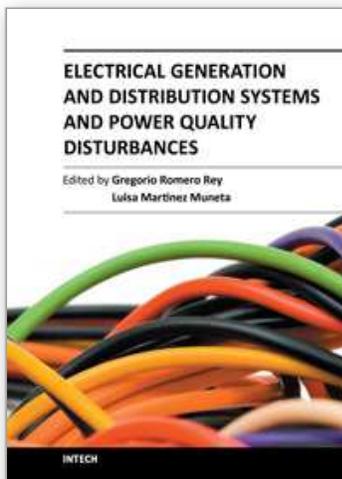
Electrical Generation and Distribution Systems and Power Quality Disturbances

Edited by Prof. Gregorio Romero

The utilization of renewable energy sources such as wind energy, or solar energy, among others, is currently of greater interest. Nevertheless, since their availability is arbitrary and unstable this can lead to frequency variation, to grid instability and to a total or partial loss of load power supply, being not appropriate sources to be directly connected to the main utility grid. Additionally, the presence of a static converter as output interface of the generating plants introduces voltage and current harmonics into the electrical system that negatively affect system power quality. By integrating distributed power generation systems closed to the loads in the electric grid, we can eliminate the need to transfer energy over long distances through the electric grid. In this book the reader will be introduced to different power generation and distribution systems with an analysis of some types of existing disturbances and a study of different industrial applications such as battery charges.

How to reference

In order to correctly reference this scholarly work, feel free to copy and paste the following:

Nopporn Patcharaprakiti, Krissanapong Kirtikara, Khanchai Tunlasakun, Juttrit Thongpron, Dheerayut Chenvidhya, Anawach Sangswang, Veerapol Monyakul and Ballang Muenpinij (2011). Modeling of Photovoltaic Grid Connected Inverters Based on Nonlinear System Identification for Power Quality Analysis, Electrical Generation and Distribution Systems and Power Quality Disturbances, Prof. Gregorio Romero (Ed.), ISBN: 978-953-307-329-3, InTech, Available from: http://www.intechopen.com/books/electrical-generation-and-distribution-systems-and-power-quality-disturbances/modeling-of-photovoltaic-grid-connected-inverters-based-on-nonlinear-system-identification-for-power

INTECH
open science | open minds